

Investigation on the Effect of Reciprocating Sliding Wear Test for Titanium Alloy, Ti-6Al-4V under Frequency Set Up

Dalila Harun^{1*}, A L Mohd Tobi², Saifulnizan Jamian³

^{1,2}Faculty of Engineering Technology, Universiti Tun Hussein Onn Malaysia, Pagoh Campus, Edu Hub Pagoh, KM1, Jalan Panchor, 84600 Pagoh, Johor, Malaysia.

dalila@uthm.edu.my, almohdtobi@gmail.com,

³Faculty of Mechanical and Manufacturing Engineering, Universiti Tun Hussein Onn Malaysia, Malaysia. saifulnz@uthm.edu.my

ABSTRACT

Reciprocating sliding wear test of uncoated titanium alloy, Ti-6Al-4V is investigated using pin-on-flat arrangement under variables of reciprocal frequency set up (1, 2 and 2.5 Hz) for contact pin Ø6.5 mm. Frictional force resulted 60 – 80 N tangential force in range and the graph pattern for COF resulted running-in condition at earlier second and highest peak experienced in value 0.45-0.48 in range. The micrography shows more sticking at the end of the wear track and significant at parameter 1 Hz frequency. The profilometry shows the result of wear width and wear area where the wear width is increasing with the increasing of frequency set up while wear area decreasing with the increasing of frequency. The hardness shows high value for 2.5 Hz. The cyclic plasticity presence is examined using Scanning Electron Microscope (SEM). The black spot present at the end of wear track are identified as an accumulation of ploughing during sliding and approved by the hardness result where the accumulation part experienced highest value 962 HV. This value proved that plastic deformation is formed during the sliding with the adhesive and abrasive mechanism.

Key words: Reciprocan frequency, reciprocating sliding wear, Titanium Alloy, Ti-6Al-4V.

1. INTRODUCTION

Titanium alloy, Ti-6Al-4V has been of great interest in recent years because of their very attractive combination of high strength, low density and corrosion resistance [1], [2]. High performance of aero engine components experienced material wear losses resulting not only reduction to its performance but in some cases a complete failure of the components. Currently there is a limitation on life prediction of aero engine components due to inability to accurately predict the wear behavior for the components due to plasticity type deformation occurring on the contact pair [3].

Sliding wear can be occurred when larger displacement is taken place. Reciprocating sliding wear will induce by debris formation for larger displacement amplitudes [4]. In research finding, the reciprocating conducted by Kandeve-Ivanova [5] reported the means value of the COF was around 0.36 for Ti-6Al-4V. Mulvihill [6] suggested that friction arises from both plasticity and tangential interface adhesion. The evolution of the microstructure during sliding wear is that the coarse-grain microstructure is transformed into nanocrystalline grains, which accordingly alters the wear properties [7].

According to Harun [8], two mechanisms of plastic deformation were highlighted which are global deformation (similar to ploughing) through the asperity overlaps and shear localization along a fine zone similar to adiabatic shear band. The rapid wear can be classified as furrow wear with large spall under SEM analysis while OM observation discovered that the microstructure at the wear contact surface underwent apparent plastic deformation. Abrasive wear form due to the ploughing action by harder surface or third bodies which are debris [9]. When the hardness of the abrasive particle is lower than the specimen hardness, no abrasive wear or only mild abrasive wear occurs.

Meanwhile, when the abrasive particle is much harder or equal than the specimen, the wear capacity increases with an increase in the abrasive particle hardness. The inability to accurately predict the wear behavior of reciprocating sliding wear and the characteristic by fretting wear can be justified same with characteristic of sliding wear are the main focus on this study. Therefore, the fundamental on the behavior of cyclic plasticity under reciprocating sliding contact condition that induced plasticity type wear need to be addressed so that the interpretation of tribological parameter on friction and wear will be more accurately presented in predicting the wear mechanism involved.

2. MATERIALS AND METHODS

2.1 Specimen and Materials

The material used in this study is titanium alloy which has the properties of excellent combination of high specific strength (strength-to-weight ratio) at elevated temperature, fracture resistant characteristics, and their exceptional resistance to corrosion. Titanium and its alloys are used extensively in aerospace [10], [11]. Its composition consists of 5.5-6.75 wt% Al, 3.5-4.5% V, and the balance is Ti. The specimen machined into two different shapes rectangular flat bar with dimensions of 100 mm x 25 mm x 8 mm and cylindrical pin of $\varnothing 6.5$ mm. Surface roughness prior to testing is $Ra = 0.2\mu\text{m}$.

2.1 Tribological Test

The experiment is done using the tribometer pin-on-flat machine, (model, TR-20, by Ducom Triboinnovaters, Universiti Sains Malaysia) connected to computer monitoring with linear reciprocating slider. The cylindrical pin was set to be static body while the flat rectangular bar is moving. The test was done in dry condition at ambient air with room temperature, 25°C and normal humidity 85% with normal load applied on the cylindrical pin through lever system amounting 200 N, 100 rpm sliding speed with 20 numbers of cycles. The parameter set up was 1, 2 and 2.5 Hz reciprocating frequency. The surface of the sample was cleaned by ethanol using a soft cotton cloth to minimize foreign material [12]. The specimen was setup as Figure 1.

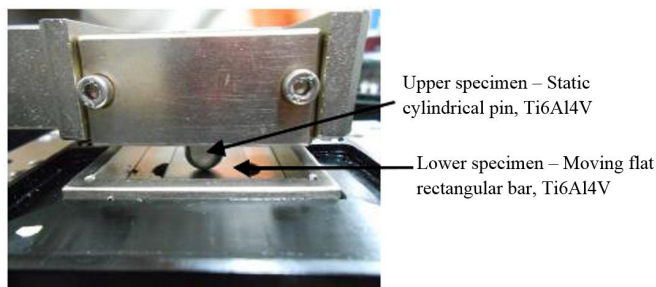


Figure 1: Arrangement of the specimen for upper and lower specimen (Harun et al., 2015)

The wear scar profilometry are examined by using 3D optical microscope (OM). The wear area is calculated by measuring wear track width and length using advanced 3D (AliCona Infinite Solution) optical microscope. The morphologies of the wear scar were observed with Scanning electron microscopy (SEM, Zeiss Evo MA, UK) system coupled. The hardness of the wear region is determined by Vicker’s Micro hardness-tester, set at load of 980.7 mN (HV0.1) indented to the surface for 5s at three different areas which are original surface, wear track and end of wear track according to ASTM E384 standard.

Table 1: Sliding test conditions for parameter of frequency

Normal load, P (N)	200 N
Frequency (Hz)	1, 2 and 2.5 Hz
Amplitude of displacement (mm)	60 mm
Cycle	20
Time/Cycle	12, 15 and 30s

3. MATERIALS AND METHODS

3.1 Frictional Force, FF

The result for the frictional force, FF against time is plotted as in Figure 2. The wear test starts with the frequency of 1 Hz and it occurred with the longest time among three parameter applied which is 30 seconds. The FF for 1 Hz shows highest value with 70 N compared to 2 and 2.5 Hz frequency with value in range 58 to 65 N, respectively. The inclined peak at maximum FF shows the formation of plastic deformation as illustrates in Figure 3 as proved by [13]. Tensile stress-strain curves of metallic alloys for Ti-6Al-4V were analyzed to investigate the working hardening behavior [4]. Once the FF increase until maximum then the flat bar just slides against the contact pin and it is clearly shows in Figure 3 that the yield strength achieved at 59 N and the ultimate strength achieved at 74 N. At this stage, the sliding occurred along the 60 mm displacement and it repeated in negative frictional force for complete back and forth linear motion or reciprocating sliding movement. During this conditions, contact part slivers extruded out laterally at the end of the wear track. The contact part access the strain hardening until it reach ultimate strength where the titanium alloy can with stand the force applied without failure. It is also called a part of partially plastic deformation occurred.

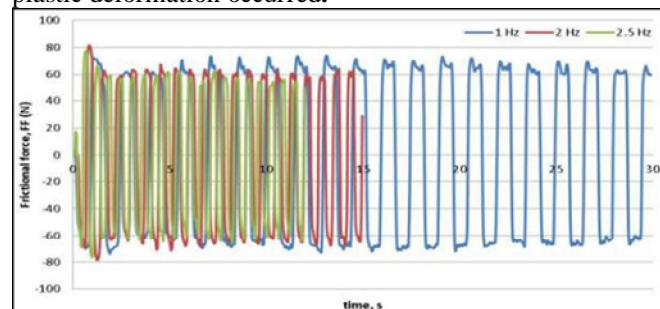


Figure 2: Frictional force, N against times, s for applied pin contact $\varnothing 6.5$ mm [applied normal load 200 N and 20 cycles]

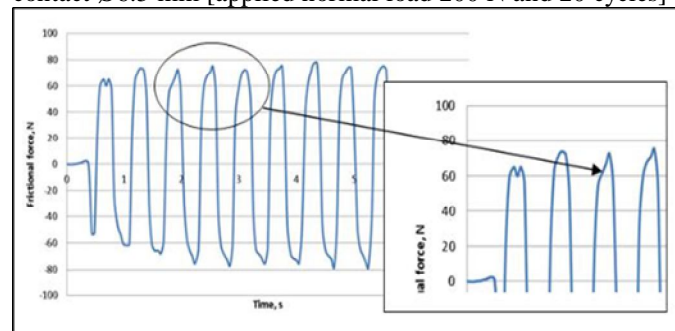


Figure 3: Maximum frictional force shows depicted uncommon peak due to the presence of plastic deformation. [20 cycles, 200 N and 2.5 Hz]

3.2 Coefficient of Friction, COF

COF result is determined directly from the monitoring computer. The frequency setup machine 1, 2 and 2.5 Hz are applied to the machine and the result for the COF against time is plotted as in Figure 4.

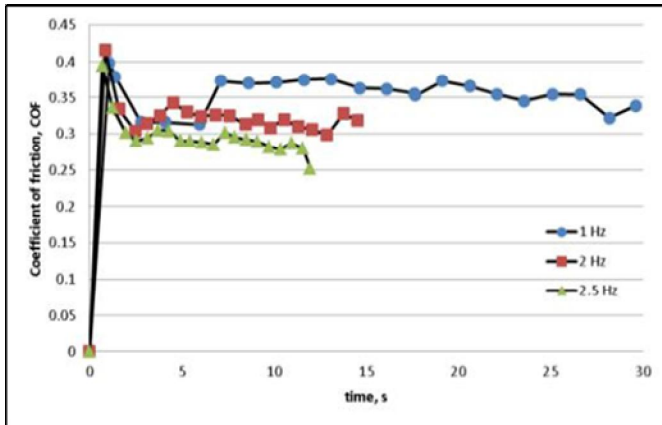


Figure 4: Coefficient of friction, COF against time, s [applied normal load 200 N and 20 cycles]

The COF for 1 Hz frequency is higher compared to 2 and 2.5 Hz frequency. COF for contact pin Ø6.5 mm was not stable in early second until 7 seconds due to high contact pressure applied during sliding and cause more plastic deformation but stable continuously then.

3.3 Micrography of The Wear Scar

Optical Microscope was used to determine the micrograph of the wear scar after the sliding test. The wear width of the wear track is determined and tabulated to characterize towards different parameter setup. Figure 5 shows an isometric view and top view of the specimen and Figure 6 represent micrograph for each variable number of frequency.

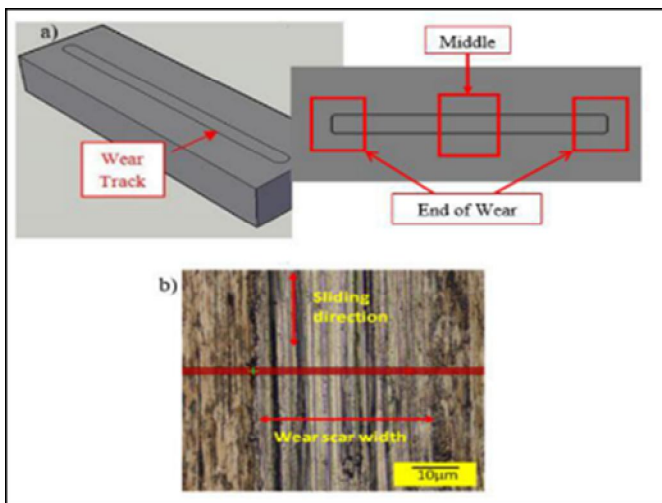


Figure 5: (a) Isometric view of the specimen and the end of the wear track and (b) 2D micrograph on wear track shows the wear scar width.

Observed that the widths of the wear track for 2.5 Hz frequency wider compared to 1 and 2 Hz. The low frequency causing more sticking or black spot especially at the left and right ends instead of less sticking form for the high frequency. The assumption made before, it was an accumulation of wear debris caused by the reciprocating sliding wear. The mechanism characterized is adhesively joined asperities that noted by Gleaser [14] and Magaziner [15], supported sliding motion occurred, to move the two surfaces, it requires breaking the adhesive bond or shearing subsurface material and the results lead to transfer material from one surface to the other.

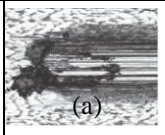
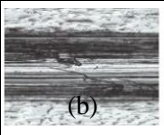
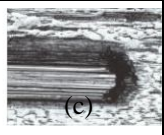
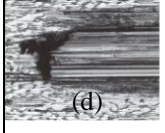
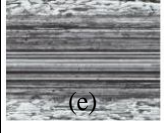
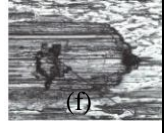
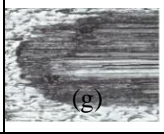
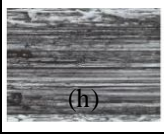
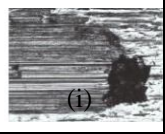
Freq. (Hz)	Left end	Middle	Right end
1			
2			
2.5			

Figure 6: Wear scar micrograph on three positions a) - c) 1 Hz, d) - f) 2 Hz, and g) - i) for 2.5 Hz, [20 cycles and 200 N applied normal load]

3.4 Profilometry, Wear Width and Wear Area Analysis

The compilation for those three profilometry for frequency set up is shown in Figure 7. Those three profilometry forms a W-shape. The wear depth is obviously high for about 14 µm for low frequency, followed by 2 Hz in the range 12 µm and lesser depth for 2.5 Hz at about 8 µm. During sliding, low frequency run for longer time therefore the wear scar groove went deeply compared to high frequency set up. The wear width and wear area data also measured from the profilometry and showed in Figure 8. It is observed that when the number of frequency increases, the wear width also increases due to the time taken during sliding where 1 Hz will take 30 seconds to complete 20 cycles and it caused high wear as compared to the results with 2 Hz and 2.5 Hz frequency.

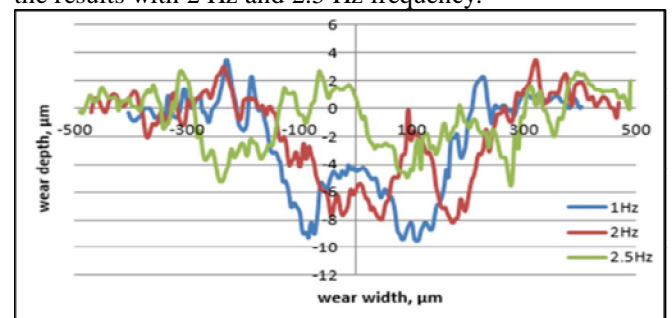


Figure 7: Wear profilometry surface for 1, 2 and 2.5 Hz frequency set up, [20 cycles and 200 N applied normal load].

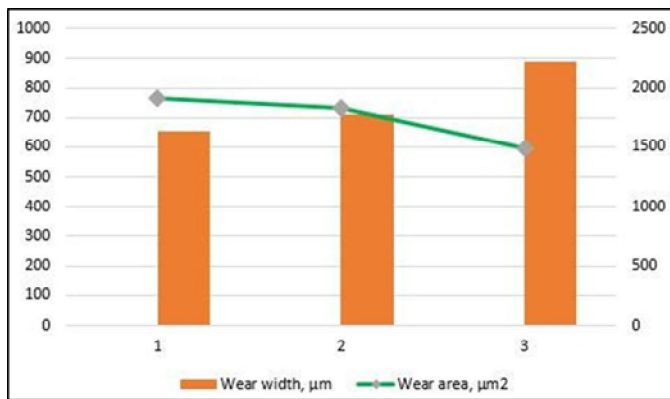


Figure 8: Wear width, µm and wear area against frequency, Hz [20 cycles and 200 N applied normal load].

3.5 Vicker’s Micro Hardness

Micro hardness results are spotted at three region area which are unworn area, middle of worn area and end of worn area as shown in Figure 9. On the other hand, Figure 10 shows the bar graph of the hardness value against the frequency set up respectively. The hardness value increases with increasing number of frequency and the hardness is higher at the end of wear track compared at the worn and unworn areas.

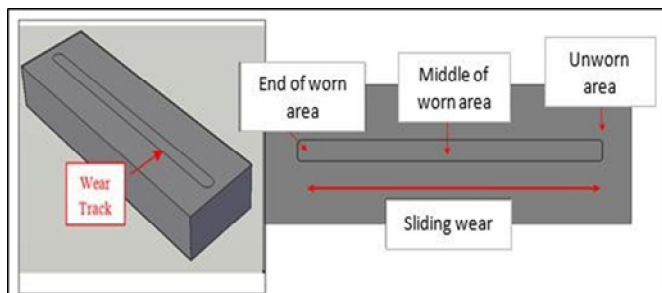


Figure 9: Schematic on isometric view of the flat specimen and the top view shows wear track resulted by the reciprocating sliding wear test and declaration of region spotted for Vicker’s Micro Hardness testing

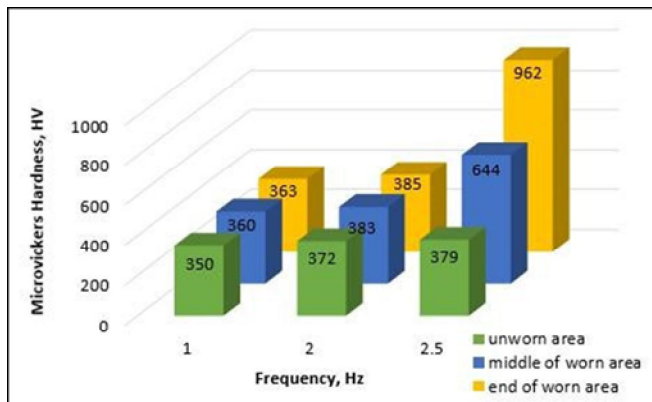


Figure 10: Hardness result on three regions spotted for three variables frequency applied contact pin Ø 6.5 mm. [20 cycles and 200 N applied normal load]

Worn surface experienced hardness value in the range of 360 – 644 HV and it increases slightly with increasing number of frequency. Same cases to the indentation area at the end of wear track where the hardness is increasing in the range of 363 – 962 HV where the value of hardness turns out to be quite high for 2.5 Hz frequency. This result can be discussed by referring to the result of micrography where the sticking of black spot is obviously formed at low frequency of 1 Hz at the location both left and right end of the wear track. This sticking clearly shows that the accumulation of plasticity has not yet formed the wear debris so the wear width, wear area and the hardness are still low as compared to high frequency 2.5 Hz. At high frequency, the plasticity accumulation completely turns into wear debris therefore less sticking formed especially at the end left and right of the wear track [3].

3.6 SEM Analysis

SEM analysis focused for 1 Hz frequency set up due to extra formation of black spots that indicates sticking or accumulation of wear then the experiment proceeded with EDX analysis. Figure 11 shows the microstructure where four spot areas were analyzed. Worn morphology presence was observed on grooves area and at the end of wear track. The general wear pattern seems to be ploughing out of the material from the worn surface. Morphology at the worn surface exhibited rough surface appearance as a result of the reciprocating sliding wear. The plastic deformation occurred at the edges of grooves and more profoundly at the end of wear track.

Magaziner [15] has supported the result of this occurrence of plastic deformation where a large amount of plastic deformation occurred in the contact zone. It can be discussed that shear stress has pushed the substrate material out of the scar that has collected at the edge of the scar. Cyclic plasticity was produced when the material lost its ductility due to strain hardening. These micrographs indicate the dominant adhesive wear in the early part of sliding, which caused severe adhesion preceded plastic deformation. This adhesive wear mechanism changed to abrasion in the later part of the test caused by the three-body abrasion due to work hardened wear particles. Severe plastic deformation can be explained based on Figure 11 (c) and (d). Typical adhesive traces and abrasive furrows, relatively rougher, with many ripped regions and abrasive furrows are briefly described by Chauhan & Dass [16]. The general wear pattern seems to be ploughing out of the material from the worn surface. The grooves on the worn surface were coarse and the plastic deformation at the edges of grooves was heavy thus resulting in higher hardness value as mentioned previously.

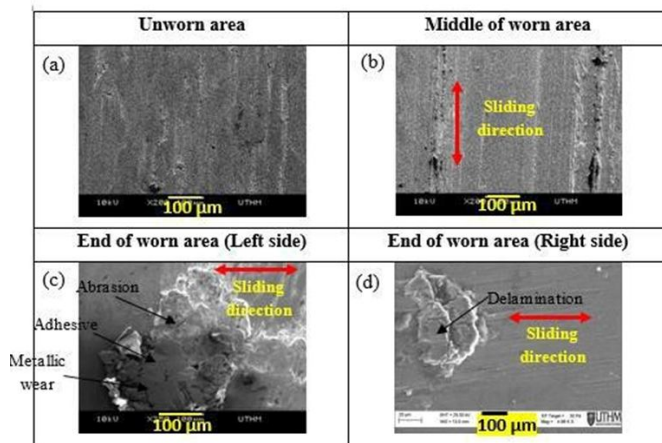


Figure 11: SEM micrographs on four spot surfaces of flat bar specimen Ti-6Al-4V at (a) unworn area, (b) middle of worn area, (c) left end of worn area and (d) right end of worn area for 1 Hz frequency

5. CONCLUSION

The frictional force results shows increasing trend and it is fluctuating constantly until the reciprocating sliding wear test was completed for those three parameters setup. The amplitude of the wavelength cycle has less significant difference as the frictional force increases up to 80 N and decreases in a range of 60-80 N.

COF value increasing with decreasing value of frequency set up. It is because the sliding wear has longer time to slides for low frequency compared to the high frequency. The wear width also shows a pattern of increasing with the increasing of frequency while the wear area are decreasing with the increasing frequency. For the hardness value, high hardness shows for 2.5 Hz with 962 HV. Increasing frequency will increase the hardness at each indentation location. Examining the presence of cyclic plasticity deformation during reciprocating sliding wear, those three positions have provided a good insight to the behavior of the wear track. The presence of adhesive and abrasive wear on the wear track. This result has been discussed by Long and Rack, (2001) as they matches the severe surface plastic deformation and transfer as commonly observed at the end of sliding pass.

ACKNOWLEDGEMENT

The authors acknowledge the financial support by the Universiti Tun Hussein Onn Malaysia (Short Term Grant Scheme No. U382).

REFERENCES

(Periodical style)

1. M. Buciumeanu, A. Araujo, O. Carvalho, G. Miranda, J. C. M. Souza, F. S. Silva and B. Henriques. **Study of the tribocorrosion behaviour of Ti6Al4V-HA**

2. G. D. Revankar, R. Shetty, S. S. Rao and V. N. Gaitonde. **Wear resistance enhancement of titanium alloy (Ti-6Al-4V) by ball burnishing process.** *Journal of Materials Research and Technology*, vol. 6, no. 1, pp. 13-32, Jan 2017.
3. A. M. Tobi, W. Sun and P. H. Shipway. **Evolution of plasticity-based wear damage in gross sliding fretting of a Ti-6Al-4V non-conforming contact.** *Tribology International*, vol. 113, pp. 474-486, Sep 2017.
4. C. Guangxiong, Z. Zhongrong, P. Kapsa and L. Vincent. **Effect of surface topography on formation of squeal under reciprocating sliding.** *Wear*, vol. 253, no. 3-4, pp. 411-423, Aug 2002.
5. M. Kandeve-Ivanova, A. Vencl and D. Karastoyanov. **Advanced tribological coatings for Heavy-duty applications: Case studies.** Bulgarian Academy of Sciences, Institute of Information and Communication Technologies, Prof. Marin Drinov Publishing House of Bulgarian Academy of Sciences, 2016.
6. D. M. Mulvihill, M. E. Kartal, D. Nowell and D. A. Hills. **An elastic-plastic asperity interaction model for sliding friction.** *Tribology international*, vol. 44, no. 12, pp. 1679-1694, Nov 2011.
7. R. Pan, R. Ren, X. Zhao and C. Chen. **Influence of microstructure evolution during the sliding wear of CL65 steel.** *Wear*, vol. 400, pp. 169-176, Apr 2018.
8. D. Harun, A. L. Mohd Tobi and A. Singh Chaal. **Characterisation of plasticity response for reciprocating sliding wear test of Ti-6Al-4V under variables normal load.** In *Advanced Materials Research*, Vol. 1087, pp. 350-354, 2015.
9. E. O. Ezugwu and Z. M. Wang. **Titanium alloys and their machinability—a review.** *Journal of materials processing technology*, vol. 68, no. 3, pp.262-274, Aug 1997.
10. E. J. Herselman. **An investigation of sliding wear of Ti6Al4V**, Doctoral dissertation, Stellenbosch: Stellenbosch University, 2012.
11. A. Kapoor. **Wear by plastic ratchetting.** *Wear*, vol. 212, no. 1, pp. 119-130, Nov 1997.
12. A. M. Tobi, J. Ding, G. Bandak, S. B. Leen and P. H. Shipway. **A study on the interaction between fretting wear and cyclic plasticity for Ti-6Al-4V.** *Wear*, vol. 267, no. 1-4, pp. 270-282, Jun 2009.
13. C. A. O. Jun, F. G. LI and Z. K. SUN. **Tensile stress-strain behavior of metallic alloys.** *Transactions of Nonferrous Metals Society of China*, vol. 27, no. 11, pp. 2443-2453, Nov 2017.
14. W. A. Glaeser. **Characterization of tribological materials.** Momentum Press, Nov 2012.
15. R. S. Magaziner, V. K. Jain and S. Mall. **Wear characterization of Ti-6Al-4V under fretting-reciprocating sliding conditions.** *Wear*, vol. 264, no. 11-12, pp. 1002-1014, May 2008.

16. S. R. Chauhan and K. Dass. **Dry sliding wear behaviour of titanium (Grade 5) alloy by using response surface methodology.** *Advances in Tribology*, Jan 2013.
17. M. Long and H. J. Rack. **Friction and surface behavior of selected titanium alloys during reciprocating-sliding motion.** *Wear*, vol. 249, no. 1-2, pp. 157-167, Apr 2001.